International Journal of Environmental Science and Technology (2020) 17:3935–3946
https://doi.org/10.1007/s13762-020-02698-w

ORIGINAL PAPER

Low-cost activated carbon: characterization, decolorization, modeling, optimization and kinetics

D. Shahbazi[1,3] · S. A. Mousavi[1,2] · D. Nayeri[1,3]

Received: 12 August 2019 / Revised: 2 February 2020 / Accepted: 26 February 2020 / Published online: 9 March 2020

Abstract

Grape wood activated carbon (GWAC) as a cost-effectiveness and nontoxic adsorbent was developed for methylene blue (MB) removal from aqueous solutions. The adsorbent was characterized using SEM, BET, FTIR and pH_{ZPC}. Design of experiments, modeling and optimization of data were carried out using central composite design through response surface methodology. The effects of the main variables including initial dye concentration (100–500 mg/L), pH (3–11), contact time (10–90 min) and adsorbent dosage (0.25–12.25 g/L) on the decolorization were investigated using analysis of variance (ANOVA). The efficiency of MB removal increased to more than 98.5% with increasing pH and contact time from 3 to 11 and 10 to 90 min, respectively, under 0.25–12.25 g/L of GWAC. The experimental data were fitted to Langmuir model ($R^2 = 0.98$), and the maximum adsorption capacity (q_{max}) was 4.82 mg/g. The adsorption kinetics were well described by the pseudo-second order ($R^2 = 0.9485$). This study highlighted grape wood waste as a suitable adsorbent with high efficiency for the removal of methylene blue from water and wastewater.

Keywords Methylene blue · Wastewater · Carbon · Adsorption · Modeling · Isotherm

List of symbols

C_0	Initial concentration of MB (mg/L)
q_e	Equilibrium adsorption capacity (mg/g)
C_e	MB concentration (mg/L) at equilibrium
V	Volume of solution (L)
W	Weight of adsorbent (g)
Y	Predicted response
h	Initial adsorption rate
e	Random error
q_m	Maximum adsorption capacity reflected a complete monolayer (mg/g) in Langmuir isotherm model
K_F	Isotherm constant indicates the capacity parameter (mg/g) related to the intensity of the adsorption
R^2	Correlation coefficient
$\%R$	Percentage of adsorption process efficiency
β_0	Offset term
β_{ij}	Interaction effect
β_{ii}	Squared effect
β_i	Linear effect
x_i and x_j	Coded values of the factors
K_L	Langmuir constant or adsorption equilibrium constant (L/mg) that is related to the apparent energy of sorption

Editorial responsibility: Abhishek RoyChowdhury.

✉ S. A. Mousavi
seyyedarm@yahoo.com

[1] Department of Environmental Health Engineering, School of Public Health, and Research Center for Environmental Determinants of Health (RCEDH), Kermanshah University of Medical Sciences, Kermanshah, Iran

[2] Social Development and Health Promotion Research Center, Kermanshah University of Medical Sciences, Kermanshah, Iran

[3] Student's Research Committee, Kermanshah University of Medical Sciences, Kermanshah, Iran

Introduction

Colored wastewaters from different industries such as paper, textile, leather, printing and food products have attracted the attention of environmentalists because of adverse effects on the natural ecosystems (Asfaram et al. 2017). Researchers to limit the effects of large amount of discharged dyes into the receiving water body have attempted to develop efficient treatment methods. In this regard, different techniques such as electrocoagulation (Mahmoud et al. 2013), membranes

(Asman et al. 2012), composites (Dehghani et al. 2017), photocatalysts (Joseph and Elilarasi 2017) and adsorption were applied. Among them, adsorption because of simple, high efficiency, favorable, and less expensive is generally applied in the elimination of pollutants, especially dyes from water and wastewater (Patil et al. 2019). The results of previous studies have shown that among the adsorbents, activated carbon (AC) can be a good alternative for the removal of dye due to high efficiency (Ahmed and Theydan 2014; Njoku et al. 2014; Zhai 2014). But AC has some limitations, including high production cost for developing countries like Iran (Gokce and Aktas 2014). Therefore, researchers have attempted to find out alternate materials for preparing activated carbon. Among different materials, activated carbon from agricultural wastes because of their quality and the availability of a wide range of raw materials has been used increasingly during last decades (Yang and Qiu 2010). Many adsorbents were developed to remove dyes from aqueous solutions using agricultural wastes including banana trunk (Danish et al. 2018), olive pomace boiler ash (Marrakchi et al. 2017), walnut shells (Yang and Qiu 2010), waste tea (Gokce and Aktas 2014), coconut husk (Foo and Hameed 2012), coconut shell (Islam et al. 2017), rice straw (Zhang et al. 2016), wood millet (Ghaedi and Nasiri Kokhdan 2015) and bamboo leaves powder (Ghosh and Bandyopadhyay 2017).

Grape as a valuable agricultural product around the world was produced in Iran more than 2,900,000 ton/year from 315,000 hectare of grapevines (Hejazifar et al. 2011). The grape wood produces a large amount of wastes due to its proper growth and also its need for pruning in which their management is very costly and time-consuming. Previous studies have confirmed that different grape wastes such as stalk (Deiana et al. 2009), bagasse (Demiral and Güngör 2016), rhytidome (Hejazifar et al. 2011) and industrial processing residuals (Sayğılı and Güzel 2015) can be used for the removal of pollutants from water and wastewater. But to the best of our knowledge, there is no study that has been employed grape wood wastes for environmental remediation.

Therefore, this study was designed and performed based on different objectives including synthesizing a new and cheap adsorbent from grape wood wastes, investigating the combined effect of independent variables: initial dye concentration, pH, contact time and adsorbent dosage on the MB removal from aqueous solutions using central composite design (CCD) through response surface methodology (RSM) by Design Expert Version 11, modeling of data using analysis of variance (ANOVA) and kinetic and isotherm studies.

Materials and methods

Chemicals, reagents and solutions

All chemicals and reagents used in this study were purchased from Merck Company with analytical standards and were used without further purification. The molecular formula and molecular weight of MB were $C_{16}H_{18}N_3ClS$ and 319.85 g/mol, respectively. Figure 1 shows the chemical structure of MB with a purity degree of 98%. The stock solution of MB was prepared by dissolving 1 g in 1 L deionized water. The pH adjustment during adsorption study was carried out using sulfuric acid (1 N) and sodium hydroxide (1 N).

Preparation and characterization of adsorbent

The grape wood wastes were obtained from pruned branches, Kermanshah grapevines, Iran. The proper branches were cut (about 2 cm), washed with distilled water in order to remove any impurities and dried under sunlight for 2 h and subsequently in a hot air oven (Memmert 854, Germany) at 100 °C for 3 h. At the first step of activation, chemical activation was carried out by submerging raw materials in H_3PO_4 (85%) for 8 h. After acid leaching, the raw materials were dried at 100 °C using a hot air oven for 4 h. At the second step, thermal activation was performed by transferring materials into jugs with two small holes to sparge gases. The jugs were put in an electric furnace (Nabertherm 11/s27, Germany), and thermal activation was performed for 1 h at 750 °C. The activated material was milled and sieved through a mesh screen of 50#.

The thermally activated materials were milled and sieved through a 200-mesh screen. The grape wood activated carbon (GWAC) was studied in terms of chemical and physical properties using Fourier transform infrared spectroscopy (FTIR) (Alpha, Bruker), scanning electron microscopy (SEM) (MIRA III, Japan) and Brunauer–Emmett–Teller (BET) (BELSORP-mini II, Japan). Also, point of zero charge (pH_{ZPC}) of AC was determined by the pH drift method.

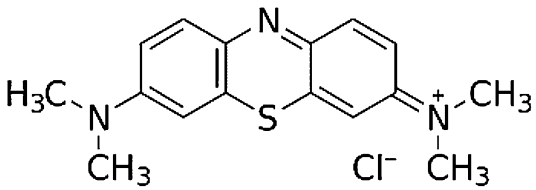

Fig. 1 Chemical structure of methylene blue

Adsorption study

This study was performed using 100 ml of methylene blue at different concentrations (100–500 mg/L) with the desired adsorbent dosage (0.25–12.25 g/L) by adjusting pH at the appropriate range of 3–11 when the contact time was adjusted at 10–90 min. The temperature was kept constant at 25 ± 2 °C during experiments. At the end of the adsorption time, the mixture was separated by a centrifuge apparatus (Shimifan, Iran). The concentration of dye was measured using an UV–Vis spectrophotometer (Jenway 6305, Germany) at a wavelength of 665 nm. The efficiency of the adsorption process was calculated based on Eq. 1 (Nayeri et al. 2019a):

$$R(\%) = \frac{C_0 - C_e}{C_0} \times 100. \quad (1)$$

Table 1 Two-level factorial of variables

Parameter name	Unit	Symbols	Low	High
Contact time	Min	X_1	10	90
pH	–	X_2	3	11
Adsorbent dosage	g/L	X_3	0.25	12.25
Initial concentration	mg/L	X_4	100	500

Experimental design and data analysis

The quantitative data can be used to create a regression model by RSM (Danish et al. 2018). Furthermore, the synergetic or antagonist effects and optimization of main factors including contact time (X_1), pH (X_2), adsorbent dosage (X_3) and the initial concentration of MB (X_4) on the MB removal can be carried out using CCD through RSM. The experiments were designed based on the coded value

Table 2 Coded and uncoded central composite design

Run no.	Parameters								Removal (%)
	Coded	X_1	Coded	X_2	Coded	X_3	Coded	X_4	
		Uncoded		Uncoded		Uncoded		Uncoded	
1	+1	90	−1	3	−1	0.25	−1	100	30.3
2	−1	10	+1	11	−1	0.25	−1	100	19.66
3	−1	10	−1	3	−1	0.25	−1	100	17
4	+1	90	+1	11	−1	0.25	−1	100	34.66
5	+1	90	+1	11	+1	12.25	−1	100	97.83
6	+1	90	−1	3	+1	12.25	−1	100	96
7	−1	10	+1	11	+1	12.25	−1	100	61.33
8	−1	10	−1	3	+1	12.25	−1	100	52.3
9	0	50	0	7	0	6.25	−0.5	200	77.5
10	0	50	+0.5	9	0	6.25	0	300	73.96
11	−0.5	30	0	7	0	6.25	0	300	56.63
12	0	50	−0.5	5	0	6.25	0	300	65.1
13	0	50	0	7	0	6.25	0	300	73.3
14	0	50	0	7	−0.5	3.25	0	300	40.4
15	0	50	0	7	+0.5	9.25	0	300	78.6
16	0	50	0	7	0	6.25	0	300	73.3
17	+0.5	70	0	7	0	6.25	0	300	68.4
18	0	50	0	7	0	6.25	+0.5	400	54.63
19	−1	10	+1	11	−1	0.25	+1	500	0
20	−1	10	−1	3	−1	0.25	+1	500	0
21	+1	90	−1	3	+1	12.25	+1	500	56.36
22	+1	90	+1	11	−1	0.25	+1	500	0
23	−1	10	+1	11	+1	12.25	+1	500	15.13
24	−1	10	−1	3	+1	12.25	+1	500	11.66
25	+1	90	+1	11	+1	12.25	+1	500	54.2
26	+1	90	−1	3	−1	0.25	+1	500	0

of the variables at five levels (Table 1), which consist of low level (− 1), central (0) and high level (+ 1). As given in Table 2, the adsorption of high concentrations of MB was performed based on the CCD with a factorial matrix of 26 steady-state runs. The results of experimental works at different runs were used to develop a predictor model (Eq. 2) using a polynomial regression model (Mousavi and Nazari 2017). Furthermore, the behavior of the adsorption system was explained using the coefficient of determination (R^2), the probability p value (95% confidence level) and other statistical parameters.

$$Y = \beta_0 + \sum_{i=1}^{k} \beta_i x_i + \sum_{i=1}^{k} \beta_{ii} x_i^2 + \sum_{i<j}^{k} \sum \beta_j x_i x_j + e. \quad (2)$$

Adsorption isotherms and kinetics

The adsorption of dye on the GWAC can be described based on experimental data using isotherm models. The isotherm studies were performed at different concentrations of dye (100–500 mg/L) when other parameters were constant (pH 7, adsorbent dosage of 6.25 g and mixing rate of 200 rpm). There are different models, the equations of which in this work are applied as given in Table 3.

The first used model (Table 3) that was developed by Langmuir assumes monolayer coating of adsorbate over a homogenous adsorbent surface (Banerjee and Chattopadhyaya 2017). The second equation was introduced by Freundlich (Table 3) as an empirical model for heterogeneous adsorbent surface (Razmi et al. 2019).

The behavior of the adsorption process was evaluated by kinetic models in different contact times (10–90 min). In this study, the pseudo-first-order and pseudo-second-order models (Ghorbani and Kamari 2019; Nekouei et al. 2015) were used to test the experimental data based on Eqs. 7–10 in Table 3 (Ghorbani and Kamari 2019; Nekouei et al. 2015).

Results and discussion

Activated carbon characterization

The physical and chemical characteristics of GWAC were determined by BET, FTIR, pH determination at zero-point charge (pH_{ZPC}) and SEM.

The BET analysis indicated that the surface area of the GWAC is 469.581 m^2/g with microporosity. The morphology of adsorbent can be assessed by SEM (Almasi et al. 2017b). The result of SEM analysis showed that the prepared activated carbon from grapevine wood has an irregular and porous shape (Fig. 2). The results of study by Hejazifar et al. (2011) showed that activated carbon prepared from grapevine rhytidome has an irregular porous structure with different sizes (Hejazifar et al. 2011).

The infrared spectra of the prepared activated carbons as a function of the activation method are represented in Fig. 3. FTIR analysis was used to determine the activated carbon functional groups before and after adsorption processes (Nayeri et al. 2019b).

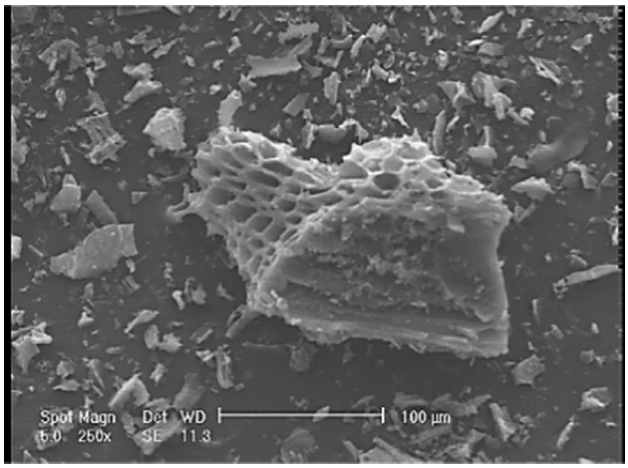

Fig. 2 SEM image of GWAC

Table 3 Isotherm and kinetics models

Models	Names	Equations	
		Linear	Nonlinear
Isotherms	Langmuir	$\frac{C_e}{q_e} = \frac{C_e}{q_m} + \frac{1}{q_m \times K_L}$ (3)	$q_e = \frac{q_m \times K \times C_e}{1 + k \times C_e}$ (4)
	Freundlich	$\log\ q_e = \log\ k_f + \frac{1}{n} \ln\ C_e$ (5)	$q_e = K_F \times C_e^{1/n}$ (6)
Kinetics	Pseudo-first order	$\log\ (q_e - q_t) = \log\ q_e - \frac{kl}{2.303} t$ (7)	$\frac{dq_t}{d_t} = k_1 (q_e - q_t)$ (8)
	Pseudo-second order	$\frac{t}{q_t} = \frac{1}{k_2 q_e^2} + \frac{1}{q_e} t$ (9)	$h = k_2 q_e^2$ (10)

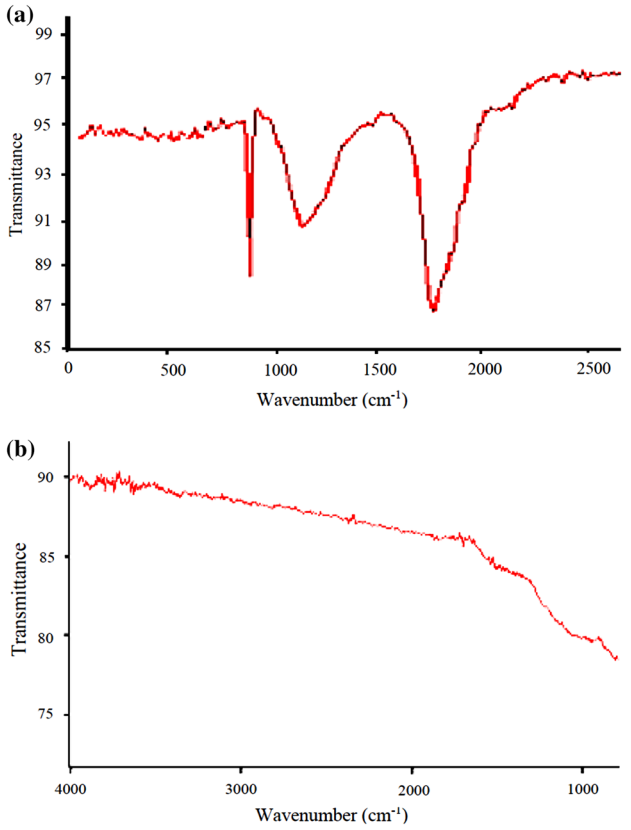

Fig. 3 FTIR spectroscopy of produced carbon before adsorption (**a**) and after adsorption (**b**)

According to Fig. 3a, the functional groups of the P–O symmetrical vibration in a chain of P–O–P (polyphosphate) are related to broadband between 900 and 1300 cm^{-1}, and also, two peaks at 1560 and 1021.74 cm^{-1} correspond to aromatic skeletal vibration and C–F group. Other studies have shown that increasing functional groups increases the dye adsorption significantly (Ekrami et al. 2016; Gupta et al. 2011). After adsorption process (Fig. 3b), the peak at about 3450 cm^{-1} was related to the –OH stretching vibration of hydroxyl functional groups, C=O stretching vibration was observed at the peak at about 1600–1700 cm^{-1}, and also the band at 2325 cm^{-1} corresponded to the C≡C stretching vibrations. Cheung et al. (2012) modified the bamboo using phosphoric acid, and they showed that carboxylic and phenolic groups were added to the surface of carbon (Cheung et al. 2012). These results are consistent with the results of studying chemical characteristics of adsorption which are obtained from vine wood (Fig. 3a, b).

In this study, the zero-point charge (pH_{ZPC}) (Fig. 4) was 5.8 for prepared activated carbon. This means that the surface charge of carbon for pH > 5.8 is negative and for pH < 5.8 is positive. Benadjemia et al. (2011) indicated that the value of zero-point charge for activated carbon

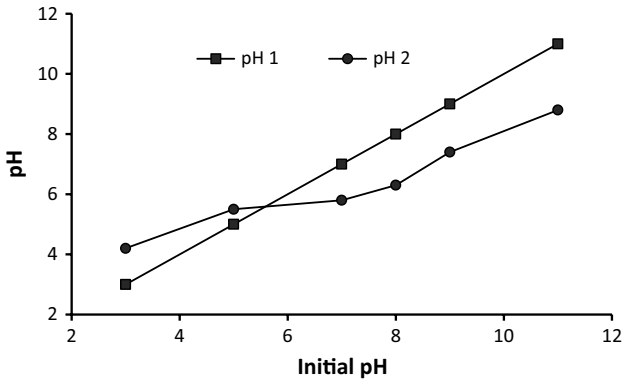

Fig. 4 pH_{ZPC} of activated carbon using phosphoric acid

produced from globe artichoke leaves using phosphoric acid at different impregnation ratios tends to neutrality as the ratio of phosphoric acid increases from 1/1 to 3/1 (Benadjemia et al. 2011).

Central composite design (CCD) and optimization of parameters

The CCD is standard RSM, which allows quadratic polynomial to be used for estimating the relationships between independent and dependent variables. Furthermore, it provides data on the interface between variables based on dependent variables (Almasi et al. 2017a). The independent variables and response for obtaining models and optimal condition include the initial MB concentration, the adsorbent dosage, contact time, pH and removal efficiency (%), which are represented in Table 2.

Multilayer regressions of experimental models based on the responses using data analysis are shown in Table 4. The larger *F*-value with the corresponding *p* value (confidence interval less than 0.05) indicates that process can be modeled successfully with less error (Elmoubarki et al. 2017). *p* values were used to determine the significant of model. The *p* value less than 0.05 shows that the effect of variable is significant (Egbuna et al. 2015). The obtained *p* value shows the significance of model. Furthermore, the *p* values of the variables show their significances. It means that both variables had effect on the MB removal efficiency ($p < 0.0001$) (Table 4). According to Table 4, since *p* values for X_1, X_2, X_3, X_4, X_1X_3, X_1X_4, X_3X_4, X_1X_2 and X_3X_2 are less than 0.05, it can be concluded that the effects of these parameters are significant statistically. The value of 219.39 for F shows that the model has a significant level. The probability is only 0.01% that the "*F*-value model" can occur due to the noise. Adeq Precision measures the signal-to-noise ratio, and also, a ratio greater than 4 is desirable (Nourani et al. 2016). In this study, obtained ratio of 47.323 indicates an adequate signal. Furthermore, the value of correlation coefficient

Table 4 Statistical analysis and modeling using DoE 8.0.0

Source	Coefficient estimate	Sum of squares	*Df*	Standard error	Mean square	*F* value	*P* value
Model	69.09	71809.36	14	0.93	5129.24	219.39	< 0.0001
X_1	12.02	7148.41	1	0.69	7148.41	305.75	< 0.0001
X_2	1.95	187.35	1	0.69	187.35	8.01	0.0062
X_3	22.12	24224.94	1	0.69	24224.94	1036.16	< 0.0001
X_4	− 14.09	9822.77	1	0.69	9822.77	420.14	< 0.0001
X_1X_2	− 0.037	0.068	1	0.70	0.068	2.887E−003	0.9573
X_1X_3	10.36	5150.16	1	0.70	5150.16	220.28	< 0.0001
X_1X_4	− 1.58	119.70	1	0.70	119.70	5.12	0.0271
X_2X_3	0.15	1.02	1	0.70	1.02	0.044	0.8352
X_2X_4	− 1.29	80.08	1	0.70	80.08	3.43	0.0689
X_3X_4	− 5.35	1371.74	1	0.70	1371.74	58.67	< 0.0001
X_1^2	− 22.71	257.29	1	6.84	257.29	11.00	0.0015
X_2^2	5.36	14.34	1	6.84	14.34	0.61	0.4364
X_3^2	− 22.31	248.30	1	6.84	248.30	10.62	0.0018
X_4^2	2.16	2.33	1	6.84	2.33	0.100	0.7532
Residual	1472.92		63	–	23.38	–	–
SD	4.84						
Mean	45.29						
C.V%	10.68						
Adeq precision	47.323						

$$\text{MB Removal } \% = +9.31375 + 1.51063\,X_1 - 3.74655\,X_2 + 10.56794\,X_3 - 0.05383\,X_4 - 0.000234\,X_1X_2 + 0.043160\,X_1X_3 - 0.000197\,X_1X_4 + 0.006076\,X_2X_3 - 0.001615\,X_2X_4 - 0.00445\,X_3X_4 - 0.014191\,X_1^2 + 0.335073\,X_2^2 - 0.619597\,X_3^2 + 0.000054\,X_4^2 \quad (11)$$

($R^2 = 0.97$) in the current study for MB removal was higher than 0.80 which shows excellent agreement between the observed results and calculated in the experiment. Moreover, the coefficient of variance (C.V) as the ratio of the standard error of estimate to the mean value of the observed response was 10.68, which can define reproducibility of the model. A model generally can be considered reproducible if its C.V is not more than 10% (Ghafari et al. 2009). From Eq. 11, it can be understood that between four main variables, adsorbent dosage and contact time have positive and significant effect on the MB removal efficiency.

In this study, in order to illustrate the correlation between the predicted values from the model calculated by Eq. 11, the plot of predicted values against actual values is shown in Fig. 5a, and the results show that the data points are distributed relatively close and have linear behavior; thus, there was sufficient agreement between the actual and the obtained data. The normal probability plot is a suitable graphical model for judging the temporary regularity (Radaei et al. 2014). Also normal probability plot showed that residuals follow the normal distribution, and in this case, the points follow a straight line. Some moderate dispersion was observed even with normal data (Egbuna et al. 2015). The defined patterns represent a response evaluation. According to normalization based on normal plot of residuals, the results were applied to determine the significance of the model using ANOVA (Fig. 5b). The obtained polynomial equation can explain the effect of main variables in greater precision when its R^2 is closer to one (Mohamadi et al. 2014). Figure 5c shows that residuals were randomly scattered around predicted values, indicating a high degree of design predictability. Figure 5d represents the Box–Cox plot for power transform and lambda versus Ln (residual SS), which shows the maximum level of the standard deviation for X was between 0 and 1. Calculating the R^2 value in this study and the results of modeling shows a good consistency.

The results in Table 4 suggest that the quadratic terms including X_3 and X_4 have the greatest effect on the MB removal. The adsorbent dosage and the initial concentration of dye are important factors on the efficiency of adsorption

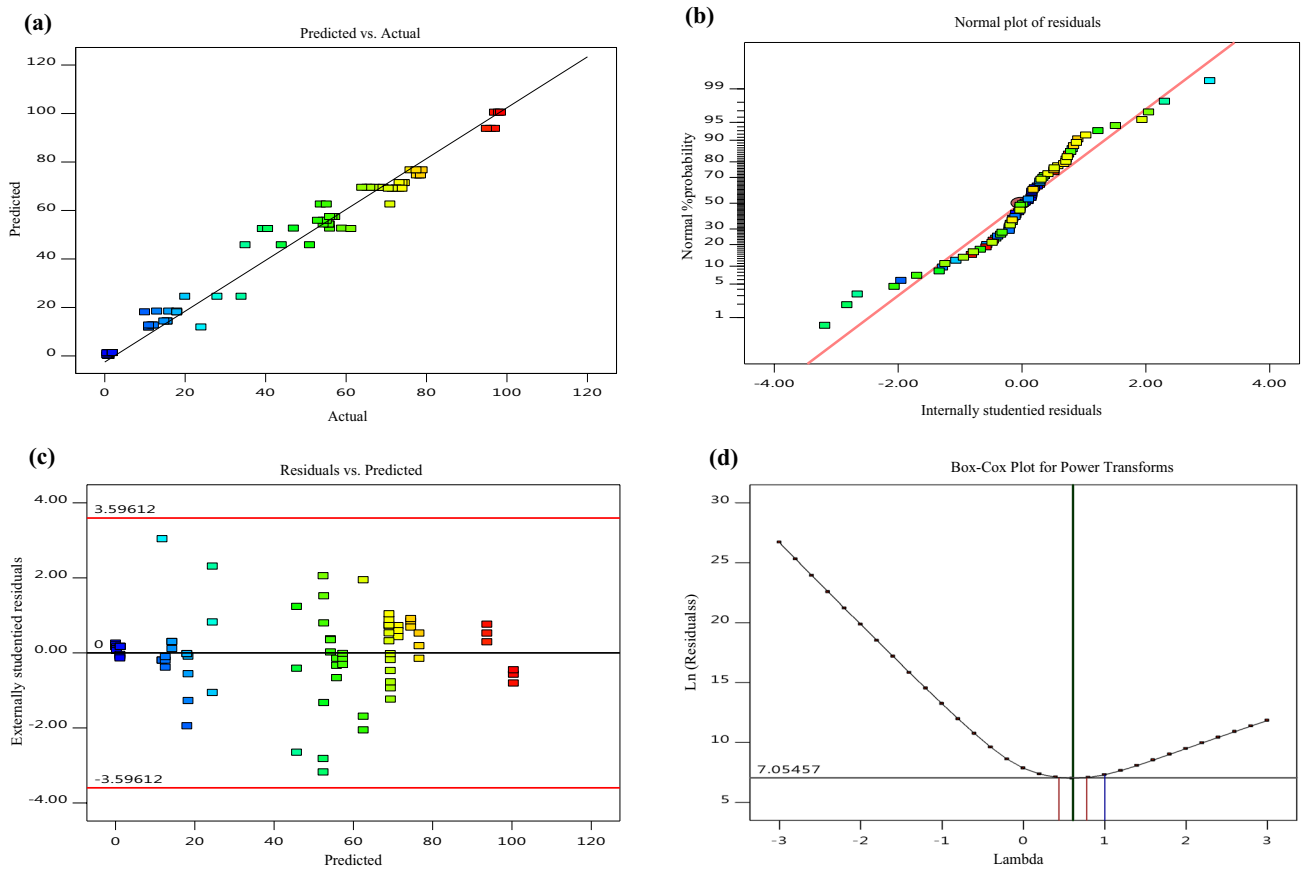

Fig. 5 **a** Predicted versus actual values plot and **b** normal probability plot, **c** residuals versus predicted and predicted versus externally studentized residuals plot and **d** Box–Cox plot for power transforms plot for MB removal

process (Etim et al. 2016). The initial concentration is an important stimulant to overcome all the resistant of transferring dye mass between soluble and solid phases (Bahramifar et al. 2015).

The surface and contour plots were used to graphically describe the behavior of adsorption system (Zhang et al. 2012) at the different values of main factors (pH value, MB concentration, adsorbent dosage and contact time) using adsorption capacity as response (Figs. 6, 7). The simultaneous effect of the adsorbent dosage and initial concentration of dye on the removal efficiency of the MB using GWAC is shown in Fig. 6. The range of adsorbent dosage varied from 0.25 to 12.25 g/L, and the initial concentration of dye varied from 100 to 500 mg/L. It was observed that by increasing the adsorbent dosage at the initial concentration of MB (100 mg/L), the removal efficiency of MB increases from 15 to 98.5%. The performed experiments showed that the maximum removal efficiency took place at the 12.25 g of adsorbent dosage and lower initial concentration of MB. A study by Orozco et al. (2018), which was investigated on the removal of MB using stems and leaves, confirmed that by increasing adsorbent dosage from 0.0125 to 0.3 g, the MB removal efficiency increased from 31 to 98.7%, respectively (Orozco et al. 2018). The same results were reported by previous studies; Nojavan and Gharbani (2017) reported that by increasing the adsorbent dosage, the efficiency of reactive blue 21 removal on its modified Kaolin increased (Nojavan and Gharbani 2017). Also, Omer et al. (2018) indicated that MB adsorption decreased as the dye concentration of the solution increased from 90 to 300 mg/L (Omer et al. 2018).

The behavior of adsorption system can be controlled by pH of solution due to the effect on the solutions chemistry, adsorbent surface charge and degree of material ionization and distribution of functional groups (Mall et al. 2005). Furthermore, the contact time as an important parameter in the adsorption process needs to be optimized. The combination effects of the contact time (10–90 min) and the pH value (3–11) at the constant value of other factors were

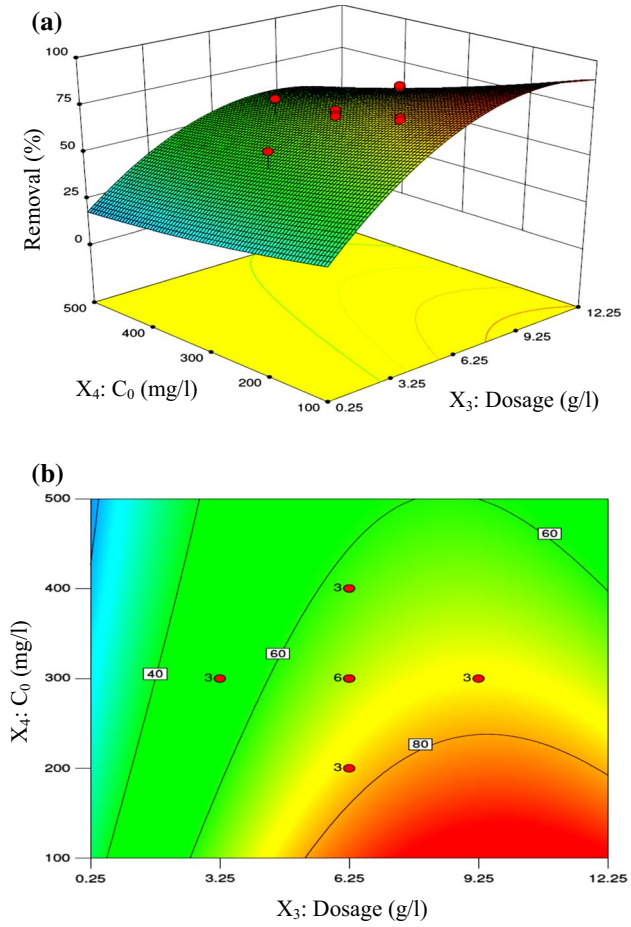

Fig. 6 **a** Three-dimensional response surface (3D) and **b** two-dimensional contour plots showing the effects of adsorbent dosage and initial MB concentration on the adsorption efficiency (pH 7 and contact time = 50 min)

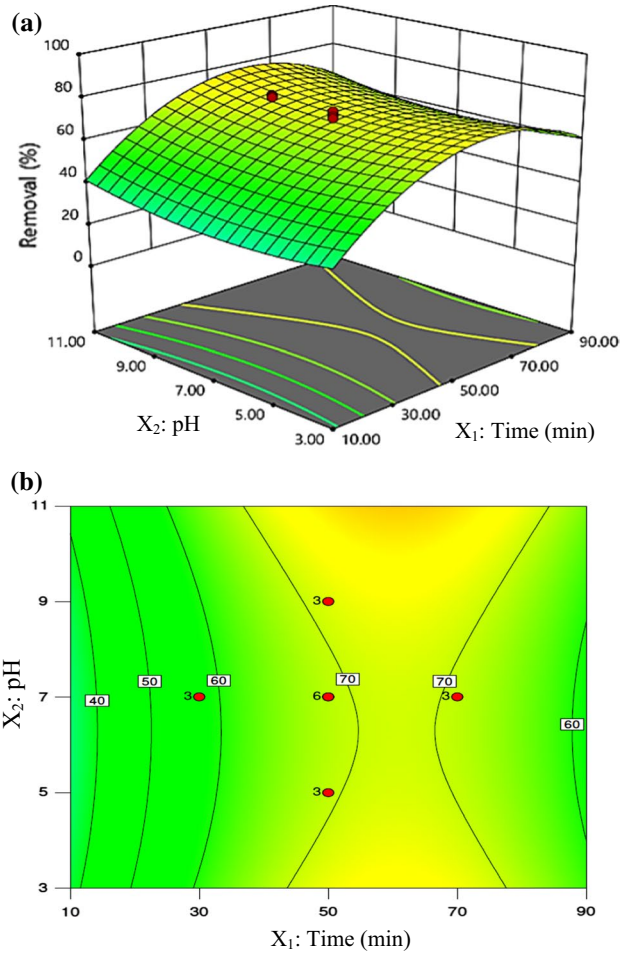

Fig. 7 **a** Three-dimensional response surface (3D) and **b** two-dimensional contour plots showing the effect of time and pH on the methylene blue removal at adsorbent dosage of 6.25 g/L and initial MB concentration of 300 mg/L

investigated. According to Fig. 7, by increasing the contact time the removal efficiency of dye increased. On the other hand, increasing pH from 5 to 9 increases the removal efficiency from 65.1 to 73.96%. In general, it was observed that increasing the contact time and pH simultaneously increases the removal efficiency of process. Kamaraj and Yamuna (2016) studied the removal of MB from aqueous solution using produced activated carbon from pineapple peel. It was observed that increasing pH from 2 to 10 increases the removal efficiency from 35.27 to 100% (Kamaraj and Yamuna 2016). Etim et al. (2016) showed that the removal efficiency of methylene blue using coconut coir dust enhanced from 94.4 to 99.2% by increasing pH from 2 to 6 (Etim et al. 2016). Al-Hussein 2017 represented increasing contact time up to maximum (to 50 min) increases the removal efficiency to 91.1% (Al-Hussein 2017). Subramaniam and Ponnusamy (2015) reported the same results (Subramaniam and Ponnusamy 2015). Hejazifar and Azizian (2012), showed that there is a significant correlation between pH and pH_{ZPC} so that in $pH > pH_{ZPC}$ the surface charge becomes negative and the removal efficiency of methylene blue (cationic dye), methyl orange and bromothymol blue (anionic dyes) increased (Hejazifar and Azizian 2012).

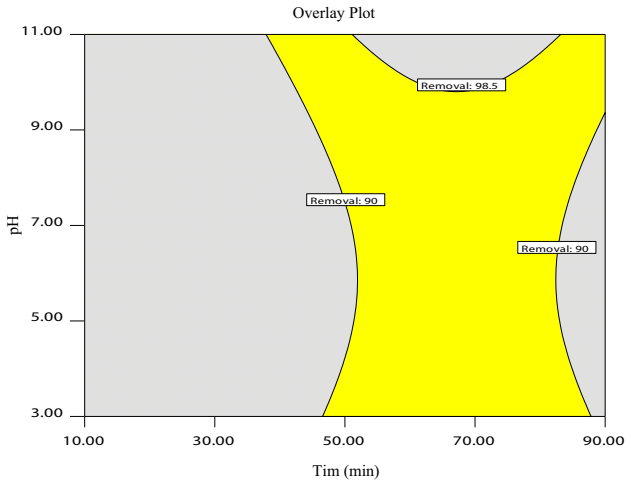

Fig. 8 Overlay plot for optimal area

Table 5 Isotherm parameters for MB adsorption using GWAC

Langmuir			Freundlich		
q_m (mg/g)	K_L (L/mg)	R^2	kf ($mg^{1-n} L^n g^{-1}$)	n	R^2
4.82	0.019	0.98	1.086	3.36	0.68

Optimization of experimental conditions

The graphical optimization provides a cover diagram for displaying areas of acceptable response values. The yellow part describes the probable conditions of the response in the operating space (Davarnejad et al. 2018). In this study, the results were optimized by Design Expert 8.0.0 by generating overlay plot (Fig. 8). Optimum conditions were achieved at pH 7 and contact time 74.42 min with removal efficiency of 94.65%.

Adsorption isotherms and kinetics

A comparison between two performed isotherm models (Table 5) showed that the equilibrium data obey Langmuir isotherm with $R^2 = 98$, which is confirmed the single-layer adsorption during the process (Ghaedi and Nasiri Kokhdan 2015). In addition, the maximum adsorption capacity (q_m) of GWAC was 4.82 mg/g. The Langmuir and Freundlich isotherm plots are shown in Fig. 9. Also, the behavior of MB adsorption was also analyzed using the pseudo-first-order and pseudo-second-order kinetics at the different contact times (10–90 min). The results showed that the pseudo-second order with R^2 of 0.948 had better performance than the pseudo-first order.

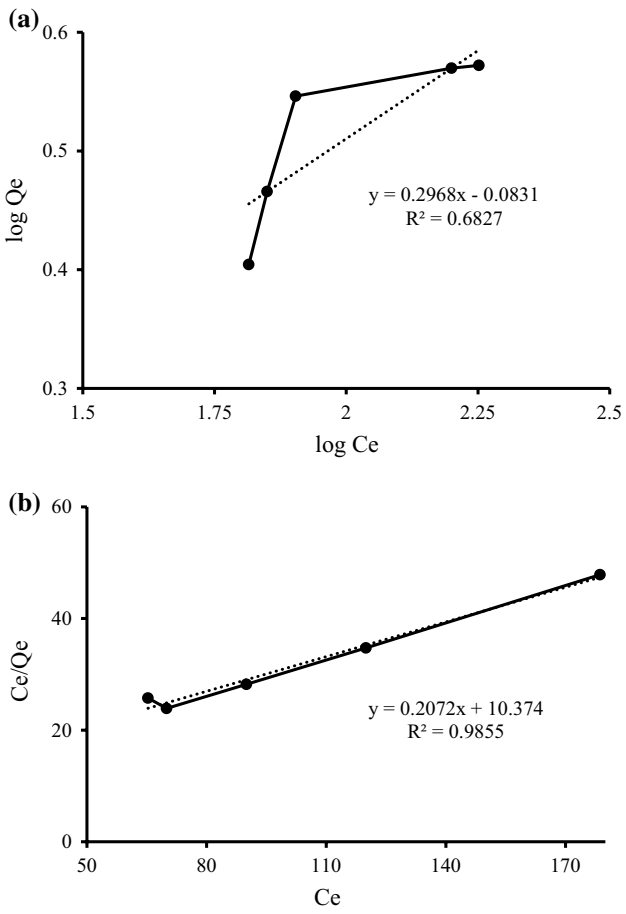

Fig. 9 Linear isotherm plots: **a** Freundlich model and **b** Langmuir models

Conclusion

In this study, the performance of AC-derived grape wood waste was evaluated for the optimization of MB removal from aqueous solution using CCD–RSM. Moreover, the impact of experimental parameters such as contact time, the initial concentration, adsorbent dosage and pH was

investigated. The obtained results showed that the maximum MB removal was 98.5% at a lower initial concentration of MB. The results confirmed that MB concentration and adsorbent dosage have the most significant effect on the process. Kinetic studies illustrated that the adsorption process was followed by a pseudo-second-order reaction with high $R^2 = 0.9485$. Different isotherm models were also employed, and the Langmuir ($R^2 = 0.98$) model was found to be great in describing the equilibrium data.

Acknowledgements The authors gratefully acknowledge the Research Council of Kermanshah University of Medical Sciences (Grant No. 94037) for the financial support. This work was performed in partial fulfillment of the requirements for master degree of Davood Shahbazi in Faculty of Health, Kermanshah University of Medical Sciences, Kermanshah, Iran.

References

Ahmed MJ, Theydan SK (2014) Optimization of microwave preparation conditions for activated carbon from *Albizia lebbeck* seed pods for methylene blue dye adsorption. J Anal Appl Pyrolysis 105:199–208. https://doi.org/10.1016/j.jaap.2013.11.005

Al-Hussein NAA (2017) Adsorption of methylene blue dye from aqueous solution by using some plants material. Mesopo Environ J 3:74–78

Almasi A, Navazeshkha F, Mousavi SA (2017a) Biosorption of lead from aqueous solution onto Nasturtium officinale: performance and modeling. Biosorption of lead from aqueous solution onto *Nasturtium officinale*: performance and modeling. Desalin Water Treat 65:443–450. https://doi.org/10.5004/dwt.2017.20308

Almasi A, Rostamkhani Z, Mousavi SA (2017b) Adsorption of reactive red 2 using activated carbon prepared from walnut shell: batch and fixed bed studies. Desalin Water Treat 79:356–367. https://doi.org/10.5004/dwt.2017.20791

Asfaram A, Ghaedi M, Hajati S, Goudarzi A, Dil EA (2017) Screening and optimization of highly effective ultrasound-assisted simultaneous adsorption of cationic dyes onto Mn-doped Fe_3O_4-nanoparticle-loaded activated carbon. Ultrason Sonochem 34:1–12. https://doi.org/10.1016/j.ultsonch.2016.05.011

Asman S, Yusof NA, Abdullah AH, Haron MJ (2012) Synthesis and characterization of hybrid molecularly imprinted polymer (MIP) membranes for removal of methylene blue (MB). Molecules 17:1916–1928. https://doi.org/10.3390/molecules17021916

Bahramifar N, Tavasolli M, Younesi H (2015) Removal of eosin Y and eosin B dyes from polluted water through biosorption using Saccharomyces cerevisiae: isotherm, kinetic and thermodynamic studies. J Appl Res Water Wastewater 2:108–114

Banerjee S, Chattopadhyaya MC (2017) Adsorption characteristics for the removal of a toxic dye, tartrazine from aqueous solutions by a low cost agricultural by-product. Arab J Chem 10:S1629–S1638. https://doi.org/10.1016/j.arabjc.2013.06.005

Benadjemia M, Millière L, Reinert L, Benderdouche N, Duclaux L (2011) Preparation, characterization and methylene blue adsorption of phosphoric acid activated carbons from globe artichoke leaves. Fuel Process Technol 92:1203–1212. https://doi.org/10.1016/j.fuproc.2011.01.014

Cheung W, Lau S, Leung S, Ip A, McKay G (2012) Characteristics of chemical modified activated carbons from bamboo scaffolding. Chin J Chem Eng 20:515–523. https://doi.org/10.1016/S1004-9541(11)60213-9

Danish M, Ahmad T, Nadhari WNAW, Ahmad M, Khanday WA, Ziyang L, Pin Z (2018) Optimization of banana trunk-activated carbon production for methylene blue-contaminated water treatment. Appl Water Sci. https://doi.org/10.1007/s13201-018-0644-7

Davarnejad R, Moraveji MK, Havaie M (2018) Integral technique for evaluation and optimization of Ni (II) ions adsorption onto regenerated cellulose using response surface methodology. Arab J Chem 11:370–379. https://doi.org/10.1016/j.arabjc.2015.05.022

Dehghani MH, Dehghan A, Najafpoor A (2017) Removing reactive red 120 and 196 using chitosan/zeolite composite from aqueous solutions: kinetics, isotherms, and process optimization. J Ind Eng Chem 51:185–195. https://doi.org/10.1016/j.jiec.2017.03.001

Deiana AC, Sardella MF, Silva H, Amaya A, Tancredi N (2009) Use of grape stalk, a waste of the viticulture industry, to obtain activated carbon. J Hazard Mater 172(1):13–19. https://doi.org/10.1016/j.jhazmat.06.095

Demiral H, Güngör C (2016) Adsorption of copper (II) from aqueous solutions on activated carbon prepared from grape bagasse. J Clean Prod 124:103–113. https://doi.org/10.1016/j.jclepro

Egbuna SO, Mbah CN, Okoye JO (2015) Optimal process parameters for the adsorption of methylene blue on thermally activated enugu white clay as a local adsorbent. Int J Eng Sci Invent 4:32–42

Ekrami E, Dadashian F, Arami M (2016) Adsorption of methylene blue by waste cotton activated carbon: equilibrium, kinetics, and thermodynamic studies. Desalin Water Treat 57:7098–7108. https://doi.org/10.1080/19443994.2015.1015173

Elmoubarki R, Taoufik M, Moufti A, Tounsadi H, Mahjoubi FZ, Bouabi Y, Qourzal S, Abdennouri M, Barka N (2017) Box–Behnken experimental design for the optimization of methylene blue adsorption onto Aleppo pine cones. J Mater Environ Sci 8:2184–2191

Etim UJ, Umoren SA, Eduok UM (2016) Coconut coir dust as a low cost adsorbent for the removal of cationic dye from aqueous solution. J Saudi Chem Soc 20:S67–S76. https://doi.org/10.1016/j.jscs.2012.09.014

Foo KY, Hameed BH (2012) Coconut husk derived activated carbon via microwave induced activation: effects of activation agents, preparation parameters and adsorption performance. Chem Eng J 184:57–65. https://doi.org/10.1016/j.cej.2011.12.084

Ghaedi M, Nasiri Kokhdan S (2015) Removal of methylene blue from aqueous solution by wood millet carbon optimization using response surface methodology. Spectrochim Acta A Mol Biomol Spectrosc 136 part B:141–148. https://doi.org/10.1016/j.saa.2014.07.048

Ghafari S, Aziz HA, Isa MH, Zinatizadeh AA (2009) Application of response surface methodology (RSM) to optimize coagulation–flocculation treatment of leachate using poly-aluminum chloride (PAC) and alum. J Hazard Mater 163:650–656. https://doi.org/10.1016/j.jhazmat.2008.07.090

Ghorbani F, Kamari S (2019) Core–shell magnetic nanocomposite of Fe_3O_4@ SiO_2@ NH_2 as an efficient and highly recyclable adsorbent of methyl red dye from aqueous environments. Environ Technol Innov 14:100333. https://doi.org/10.1016/j.eti.2019.100333

Ghosh SK, Bandyopadhyay A (2017) Adsorption of methylene blue onto citric acid treated carbonized bamboo leaves powder: equilibrium, kinetics, thermodynamics analyses. J Mol Liq 248:413–424. https://doi.org/10.1016/j.molliq.2017.10.086

Gokce Y, Aktas Z (2014) Nitric acid modification of activated carbon produced from waste tea and adsorption of methylene blue and phenol. Appl Surf Sci 313:352–359. https://doi.org/10.1016/j.apsusc.2014.05.214

Gupta V, Gupta B, Rastogi A, Agarwal S, Nayak A (2011) A comparative investigation on adsorption performances of mesoporous activated carbon prepared from waste rubber tire and activated carbon for a hazardous azo dye—acid blue 113. J Hazard Mater 186:891–901. https://doi.org/10.1016/j.jhazmat.2010.11.091

Hejazifar M, Azizian S (2012) Adsorption of cationic and anionic dyes onto the activated carbon prepared from grapevine rhytidome. J Dispers Sci Technol 33(6):846–853. https://doi.org/10.1080/01932691.2011.579861

Hejazifar M, Azizian S, Sarikhani H, Li Q, Zhao D (2011) Microwave assisted preparation of efficient activated carbon from grapevine rhytidome for the removal of methyl violet from aqueous solution. J Anal Appl Pyrolysis 92:258–266. https://doi.org/10.1016/j.jaap.2011.06.007

Islam MA, Ahmed MJ, Khanday WA, Asif M, Hameed BH (2017) Mesoporous activated coconut shell-derived hydrochar prepared via hydrothermal carbonization-NaOH activation for methylene blue adsorption. J Environ Manage 203:237–244. https://doi.org/10.1016/j.jenvman.2017.07.029

Joseph CG, Elilarasi L (2017) Removal of methylene blue dye from aqueous solution using a newly synthesized TiO_2–SiO_2 photocatalyst in the presence of active chlorine species. IOP Conf Ser Mater Sol 206:012090. https://doi.org/10.1088/1757-899x/206/1/012090

Kamaraj M, Yamuna M (2016) Pineapple peel waste activated carbon as an adsorbent for the effective removal of methylene blue dye from aqueous solution. Int J Chemtech Res 9:544–550

Mahmoud MS, Farah JY, Farrag TE (2013) Enhanced removal of methylene blue by electrocoagulation using iron electrodes. Egypt J Pet 22:211–216. https://doi.org/10.1016/j.ejpe.2012.09.013

Mall ID, Srivastava VC, Agarwal NK, Mishra IM (2005) Adsorptive removal of malachite green dye from aqueous solution by bagasse fly ash and activated carbon-kinetic study and equilibrium isotherm analyses. Colloid Surf A Physicochem Eng Asp 264:17–28. https://doi.org/10.1016/j.colsurfa.2005.03.027

Marrakchi F, Bouaziz M, Hameed BH (2017) Adsorption of acid blue 29 and methylene blue on mesoporous K_2CO_3-activated olive pomace boiler ash. Colloid Surf A Physicochem Eng Asp 535:157–165. https://doi.org/10.1016/j.colsurfa.2017.09.014

Mohamadi P, Ferina L, Suffian M, Annuar M, Ibrahim S (2014) Optimization of dye removal from aqueous Remazol Brilliant Blue R (RBBR) by Trametes sp. Pellets. J Appl Res Water Wastewater 1:1–5. https://doi.org/10.22126/arww.2014.43

Mousavi SA, Nazari S (2017) Applying response surface methodology to optimize the fenton oxidation process in the removal of reactive red 2. Pol J Environ Stud 26:765–772. https://doi.org/10.15244/pjoes/65365

Nayeri D, Mousavi SA, Fatahi M, Almasi A, Khodadoost F (2019a) Dataset on adsorption of methylene blue from aqueous solution onto activated carbon obtained from low cost wastes by chemical-thermal activation–modelling using response surface methodology. Data Brief 25:104036. https://doi.org/10.1016/j.dib.2019.104036

Nayeri D, Mousavi SA, Mehrabi A (2019b) Oxytetracycline removal from aqueous solutions using activated carbon prepared from corn stalks. J Appl Res Water Wastewater 6:67–72. https://doi.org/10.22126/arww.2019.1136

Nekouei F, Nekouei S, Tyagi I, Gupta VK (2015) Kinetic, thermodynamic and isotherm studies for acid blue 129 removal from liquids using copper oxide nanoparticle-modified activated carbon as a novel adsorbent. J Mol Liq 201:124–133. https://doi.org/10.1016/j.molliq.2014.09.027

Njoku VO, Foo KY, Asif M, Hameed BH (2014) Preparation of activated carbons from rambutan (Nephelium lappaceum) peel by microwave-induced KOH activation for acid yellow 17 dye adsorption. Chem Eng J 250:198–204. https://doi.org/10.1016/j.cej.2014.03.115

Nojavan A, Gharbani P (2017) Response surface methodology for optimizing adsorption process parameters of reactive blue 21 onto modified Kaolin. Adv Environ Technol 2:89–98. https://doi.org/10.22104/AET.2017.505

Nourani M, Baghdadi M, Javan M, Bidhendi GN (2016) Production of a biodegradable flocculant from cotton and evaluation of its performance in coagulation-flocculation of kaolin clay suspension: optimization through response surface methodology (RSM). J Environ Chem Eng 4:1996–2003. https://doi.org/10.1016/j.jece.2016.03.028

Omer OS, Hussein MA, Hussein BH, Mgaidi A (2018) Adsorption thermodynamics of cationic dyes (methylene blue and crystal violet) to a natural clay mineral from aqueous solution between 293.15 and 323.15 K. Arab J Chem 11:615–623. https://doi.org/10.1016/j.arabjc.2017.10.007

Orozco RS, Martínez-Juan M, García-Sánchez JJ, Ureña-Núñez F (2018) Removal of methylene blue from aqueous solution using typha stems and leaves. Bioresour Technol. https://doi.org/10.15376/biores.13.1.1696-1710

Patil CS, Gunjal DB, Naik VM, Harale NS, Jagadale SD, Kadam AN, Patil PS, Kolekar GB, Gore AH (2019) Waste tea residue as a low cost adsorbent for removal of hydralazine hydrochloride pharmaceutical pollutant from aqueous media: an environmental remediation. J Clean Prod 206:407–418. https://doi.org/10.1016/j.jclepro.2018.09.140

Radaei E, Moghaddam MRA, Arami M (2014) Removal of reactive blue 19 from aqueous solution by pomegranate residual-based activated carbon: optimization by response surface methodology. J Environ Health Sci Eng 12:65. http://www.ijehse.com/content/12/1/65

Razmi FA, Ngadi N, Wong S, Inuwa IM, Opotu LA (2019) Kinetics, thermodynamics, isotherm and regeneration analysis of chitosan modified pandan adsorbent. J Clean Prod 231:98–109. https://doi.org/10.1016/j.jclepro.2019.05.228

Sayğılı H, Güzel F (2015) Performance of new mesoporous carbon sorbent prepared from grape industrial processing wastes for malachite green and congo red removal. Chem Eng Res Des 100:27–38. https://doi.org/10.1016/j.cherd.2015.05.014

Subramaniam R, Ponnusamy SK (2015) Novel adsorbent from agricultural waste (cashew NUT shell) for methylene blue dye removal: optimization by response surface methodology. Water Resour Ind 11:64–70. https://doi.org/10.1016/j.wri.2015.07.002

Yang J, Qiu K (2010) Preparation of activated carbons from walnut shells via vacuum chemical activation and their application for methylene blue removal. Chem Eng J 165:209–217. https://doi.org/10.1016/j.cej.2010.09.019

Zhai QZ (2014) Nano α-Al_2O_3 for removal of Hg(II) from water: adsorption and desorption studies. J Chem Pharm Res 6:1310–1317

Zhang B, Zhang J, Yang Q, Feng C, Zhu Y, Ye Z, Ni J (2012) Investigation and optimization of the novel UASB-MFC integrated

system for sulfate removal and bioelectricity generation using the response surface methodology (RSM). Bioresour Technol 124:1–7. https://doi.org/10.1016/j.biortech.2012.08.045

Zhang S, Wang Z, Zhang Y, Pan H, Tao L (2016) Adsorption of methylene blue on organosolv lignin from rice straw procedia. Environ Sci 31:3–11. https://doi.org/10.1016/j.proenv.2016.02.001